Electronic Supplementary Information for

Significant reduction in lattice thermal conductivity in a p-type filled skutterudite due to strong electron–phonon interactions

Zhenyu Zhu[1], Jinyang Xi[1,2,*], and Jiong Yang[1,2]

[1]Materials Genome Institute, Shanghai University, 99 Shangda Road, Shanghai 200444, China.

[2]Zhejiang Laboratory, Hangzhou, Zhejiang 311100, China.

*Corresponding author: jinyangxi@t.shu.edu.cn

1. Table and Figures

Table S1 Nearest neighbor atomic numbers and lattice thermal conductivity (only including the phonon-phonon interaction) in $BaFe_4Sb_{12}$ at 300 K.

Atomic numbers	Lattice thermal conductivity (W/mK)
2	3.25
3	1.88
5	0.61
2 (Cal.[a])	3.20
Exp.[b]	2.15

a. W. Li and N. Mingo, *Phys. Rev. B*, 2015, **91**, 144304.

b. X. Shi, J. Yang, J. R. Salvador, M. Chi, J. Y. Cho, H. Wang, S. Bai, J. Yang, W. Zhang and L. Chen, *J. Am. Chem. Soc.*, 2011, **133**, 7837–7846.

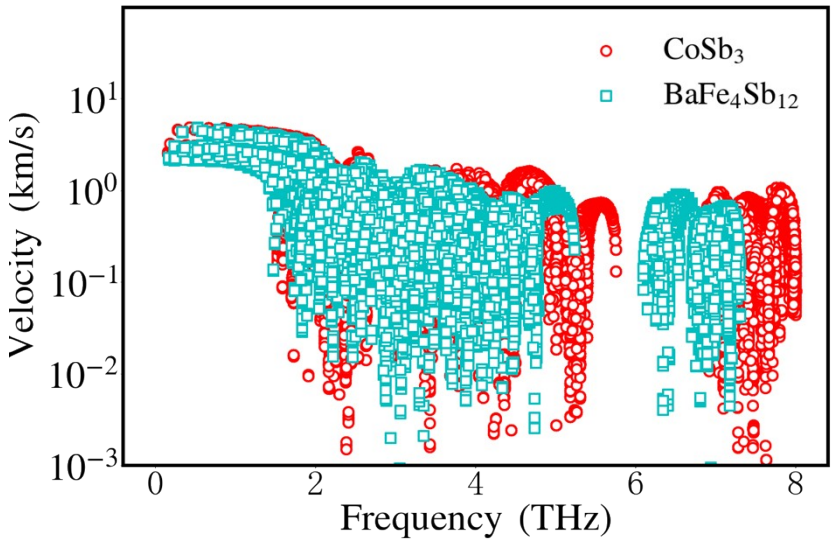

Fig. S1 Phonon group velocity as a function of frequency in $CoSb_3$ and $BaFe_4Sb_{12}$, respectively.

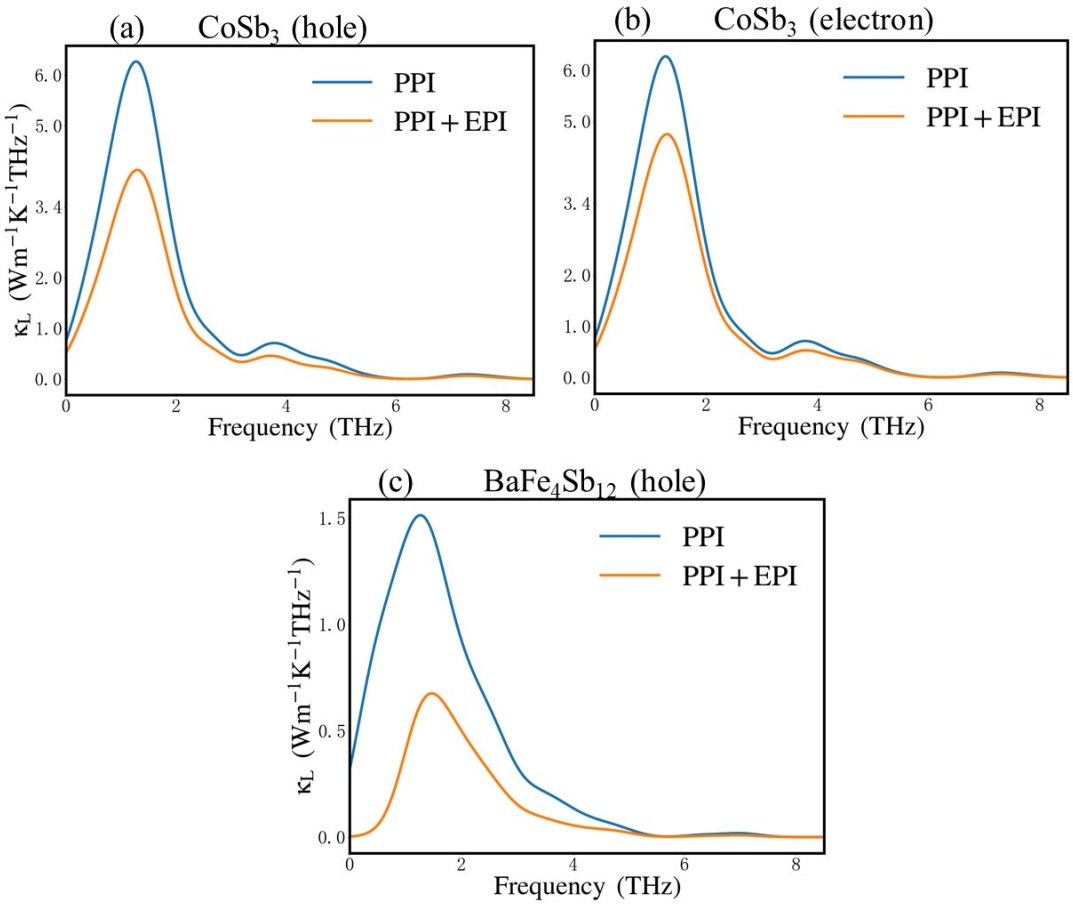

Fig. S2 Lattice thermal conductivity κ_L as a function of phonon frequency at 300 K as considering only PPI (blue line) and both PPI and EPI (orange line) in $CoSb_3$ (10^{21} cm^{-3} doping of (a) hole and (b) electron) and (c) $BaFe_4Sb_{12}$ (5×10^{21} cm^{-3} hole doping), respectively.

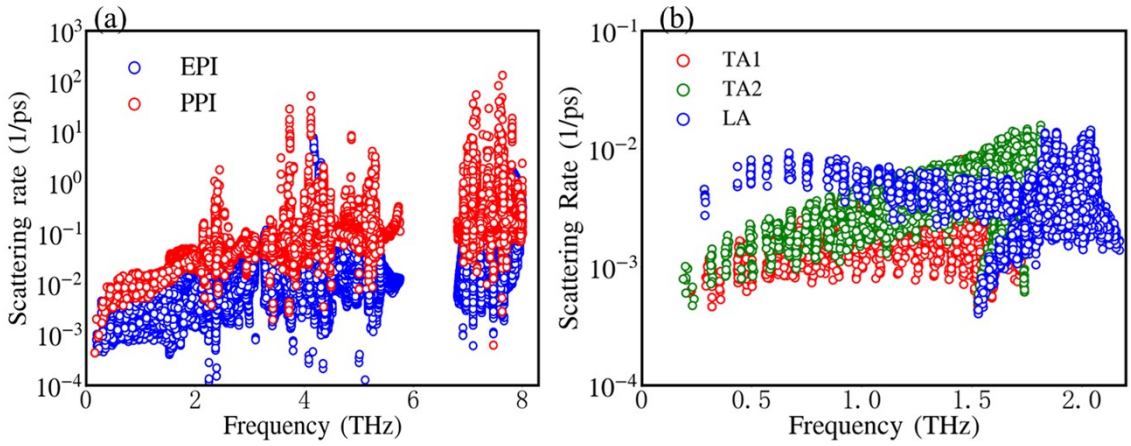

Fig. S3 (a) Phonon scattering rates from the PPI (red hollow dots) and EPI (blue hollow dots) at 300 K for $CoSb_3$ with an electron concentration 10^{21} cm^{-3}; (b) EPI scattering rates (300 K) of three acoustic phonon modes for $CoSb_3$ with an electron concentration 10^{21} cm^{-3}.

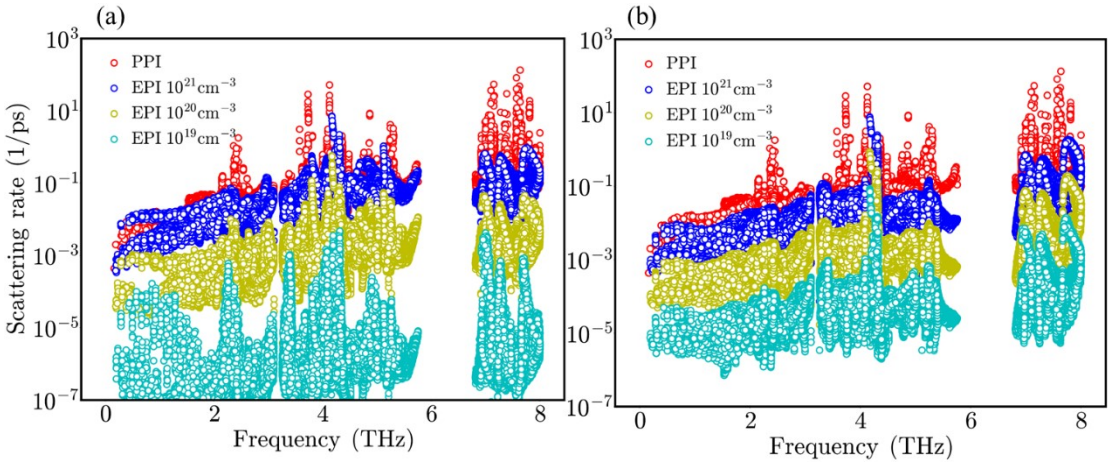

Fig. S4 Phonon scattering rates from the PPI (red hollow dots) and EPI at 300 K for $CoSb_3$ with (a) hole and (b) electron concentrations: 10^{21} cm^{-3} (blue hollow dots), 10^{20} cm^{-3}(yellow hollow dots) and 10^{19} cm^{-3}(cyan hollow dots).

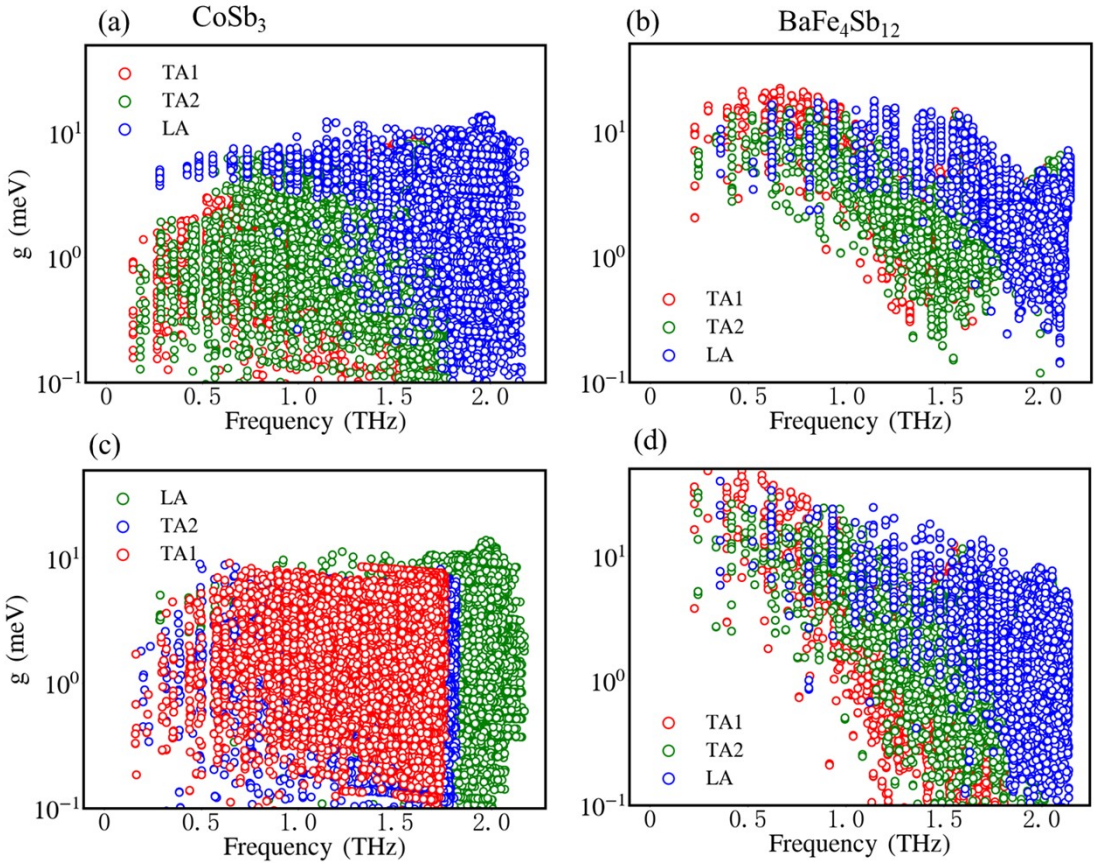

Fig. S5 TA1/TA2/LA phonon frequency dependent EPI matrix element *g* for valence band with the initial electron state at (a) **H** point for $CoSb_3$, (b) **H** point for $BaFe_4Sb_{12}$, (c) **N** point for $CoSb_3$ and (d) **N** point for $BaFe_4Sb_{12}$, respectively.

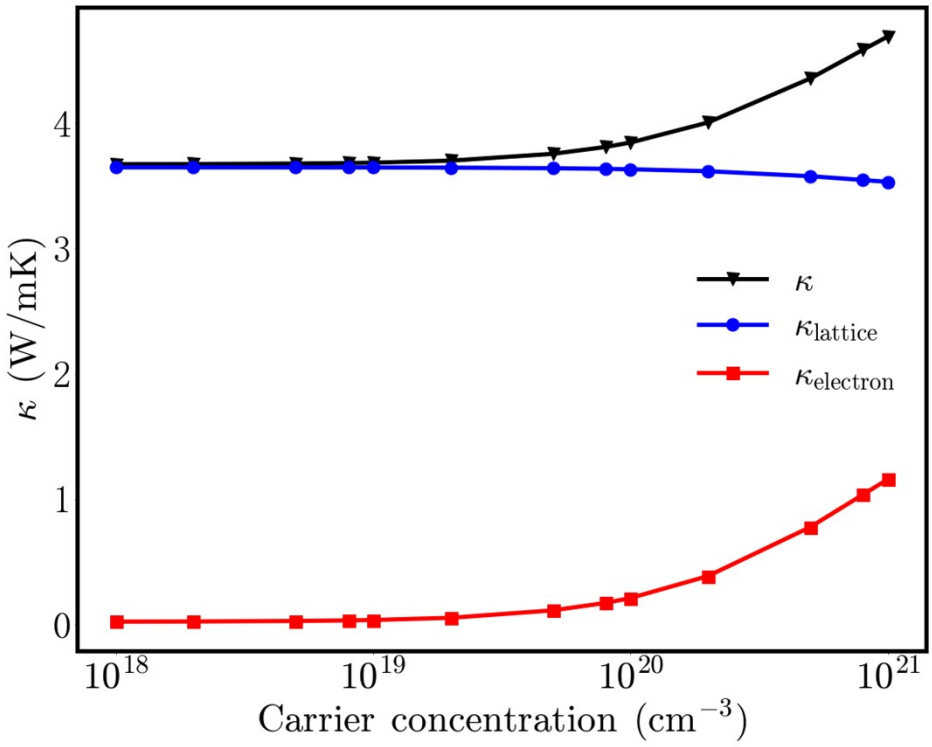

Fig. S6 Thermal conductivity κ as a function of electron concentration at 850 K in $CoSb_3$. The black line represents the total thermal conductivity, the blue line represents the lattice thermal conductivity as considering both PPI and EPI, and the red line represents the electronic thermal conductivity.

2. Methods

2.1 Anharmonic effect

In order to consider the anharmonic effect in second- and third-order interatomic force constants (IFCs) for lattice thermal conductivity, the *ab initio* molecular dynamics (AIMD) simulation and temperature dependent effective potential (TDEP)[1,2] calculation are performed in $BaFe_4Sb_{12}$. The AIMD simulation is employed by using Vienna *ab initio* simulation package (VASP).[3,4] The supercell of 3×3×3 and energy cutoff of 300 eV are used. The Brillouin zone integration is carried out by only **Γ** point. The AIMD simulation is in the canonical ensemble at 300 K and under the PBE functional, which controlled by the Nose-Hoover thermostat. The simulation time is 40 ps with a time step of 2 fs, and the initial 6 ps's information is excluded due to the nonequilibrium. In the calculations of second- and third-order IFCs by TDEP, the cutoff distance of interatomic forces is set as 10 Å and 5 Å respectively. Finally, we use the anharmonic IFCs to calculate the lattice thermal conductivity by ShengBTE code.[5]

2.2 Four-phonon scattering

In order to consider the four-phonon scattering effect on the lattice thermal conductivity of $BaFe_4Sb_{12}$, the fourth-order IFCs should be first determined. Based on the AIMD simulation at 300 K (details are given in the part 2.1), the Hiphive code[6,7] is employed to obtain the fourth-order IFCs, and the cutoff distance of interatomic forces is set as 3 Å. Notably, the second- and third-order IFCs are come from the above TDEP calculations, and the anharmonic effect is included in all the IFCs. Then, the phonon-phonon interaction (PPI) scattering rate for the four-phonon process can be determined by the following equations:[8]

$$\Gamma^{++}_{\lambda\lambda'\lambda''\lambda'''} = \frac{\hbar^2\pi(1+n')(1+n'')n'''\delta(\omega+\omega'+\omega''-\omega''')}{8N \quad n \quad \omega\omega'\omega''\omega'''}\left|V^{++}_{\lambda\lambda'\lambda''\lambda'''}\right|^2, \tag{1}$$

$$\Gamma^{+-}_{\lambda\lambda'\lambda''\lambda'''} = \frac{\hbar^2\pi(1+n')n''n'''\delta(\omega+\omega'-\omega''-\omega''')}{8N \quad n \quad \omega\omega'\omega''\omega'''}\left|V^{+-}_{\lambda\lambda'\lambda''\lambda'''}\right|^2, \tag{2}$$

$$\Gamma^{--}_{\lambda\lambda'\lambda''\lambda'''} = \frac{\hbar^2\pi n'n''n'''\delta(\omega-\omega'-\omega''-\omega''')}{8N \quad n \quad \omega\omega'\omega''\omega'''}\left|V^{--}_{\lambda\lambda'\lambda''\lambda'''}\right|^2, \tag{3}$$

where $V^{\pm\pm}_{\lambda\lambda'\lambda''\lambda'''}$ is the four-phonon scattering matrix element. Combining with the PPI scattering rate for the three-phonon process, we can obtain the total PPI scattering rate. Finally, the lattice thermal conductivity of $BaFe_4Sb_{12}$ at 300 K is calculated by using the ShengBTE code[5] with 10×10×10 mesh.

2.3 Electronic thermal conductivity

Based on the Boltzmann transport theory and relaxation time approximation, the electrical conductivity σ, Seebeck coefficient S and electronic thermal conductivity κ_e at temperature T can be expressed as follows:[9]

$$\sigma_{\alpha\beta}(\varepsilon_F,T) = \frac{1}{N_k\Omega}\sum_{nk} v^{\alpha}_{nk} v^{\beta}_{nk} \tau_{nk}\left[-\frac{\partial f_{nk}(\varepsilon_F,T)}{\partial \varepsilon_{nk}}\right], \quad (4)$$

$$S_{\alpha\beta}(\varepsilon_F,T) = \frac{1}{eTN_k\Omega}\sigma_{\alpha\beta}(\varepsilon_F,T)^{-1}\sum_{nk} v^{\alpha}_{nk} v^{\beta}_{nk} \tau_{nk}(\varepsilon_{nk}-\varepsilon_F)\left[-\frac{\partial f_{nk}(\varepsilon_F,T)}{\partial \varepsilon_{nk}}\right], \quad (5)$$

$$\kappa^{\alpha\beta}_{e}(\varepsilon_F,T) = \frac{1}{N_k\Omega}\sum_{nk}\frac{(\varepsilon_{nk}-\varepsilon_F)^2}{T} v^{\alpha}_{nk} v^{\beta}_{nk} \tau_{nk}\left[-\frac{\partial f_{nk}(\varepsilon_F,T)}{\partial \varepsilon_{nk}}\right] - T(S^2\sigma)_{\alpha\beta}(\varepsilon_F,T), \quad (6)$$

where α and β are the directions, $N_{\mathbf{k}}$ is the number of **k** points, Ω is the volume of unit cell, $\varepsilon_{n\mathbf{k}}$, $f_{n\mathbf{k}}$, and $\boldsymbol{v}_{n\mathbf{k}}$ are the electronic energy for band-index n and wave-vector **k** and corresponding Fermi-Dirac distribution and group velocity, respectively. The ε_F is the Fermi energy and e is the electron charge. τ is the electron relaxation time. If only considering the intrinsic electron-phonon scatterings, τ is expressed as:[9]

$$\frac{1}{\tau_{nk}} = \frac{2\pi}{\hbar}\sum_{mq\lambda}|g_{mn\lambda}(k,q)|^2\{(f_{mk+q}+n_{q\lambda})\delta(\varepsilon_{mk+q}-\varepsilon_{nk}-\hbar\omega_{q\lambda}) + (1+n_{q\lambda}-f_{mk+q})\delta(\varepsilon_{mk+q}-$$
$$\}$$

(7)

Here, n and ω are the Bose-Einstein distribution of phonon and frequency with branch λ and wave-vector **q**, respectively.

For $CoSb_3$, we first calculate the electronic relaxation time τ in Eq. (7) by using Quantum Espresso (QE)[10] package and EPW code.[11] The computational details are as the same as those of lattice thermal conductivity calculation. Then, the electrical transport parameters in Eqs. (4-6) at different electron concentrations can be obtained

by using our developed TransOpt code.[12] Finally, the total thermal conductivity at 850 K is combined by the electronic and lattice ones. The reason of choosing 850 K is that the thermoelectric performance of *n*-type $CoSb_3$ at this temperature is best.[13] Differently, the electrical conductivity σ of $BaFe_4Sb_{12}$ comes from the experiment with the value of 3.08×10^5 S/m at 300 K,[14] and the κ_e is estimated as according to the Wiedemann–Franz law: $\kappa_e = LT\sigma$. L is the Lorenz number with the value of 3.29×10^{-8} V^2/K^2 at 300 K, which is obtained by our calculation under the constant electron-phonon interaction approximation.[12]

References

1. O. Hellman and I. A. Abrikosov, *Phys. Rev. B*, 2013, **88**, 144301.
2. O. Hellman, I. A. Abrikosov and S. I. Simak, *Phys. Rev. B*, 2011, **84**, 180301.
3. P. E. Blöchl, *Phys. Rev. B*, 1994, **50**, 17953–17979.
4. G. Kresse and J. Furthmüller, *Phys. Rev. B*, 1996, **54**, 11169–11186.
5. W. Li, J. Carrete, N. A. Katcho and N. Mingo, *Comput. Phys. Commun.*, 2014, **185**, 1747–1758.
6. F. Eriksson, E. Fransson and P. Erhart, *Adv. Theory Simul.*, 2019, **2**, 1800184.
7. E. Fransson, F. Eriksson and P. Erhart, *npj Comput. Mater.*, 2020, **6**, 135.
8. Z. Han, X. Yang, W. Li, T. Feng and X. Ruan, *Comput. Phys. Commun.*, 2022, **270**, 108179.
9. J. Ding, C. Liu, L. Xi, J. Xi and J. Yang, *J. Materiomics*, 2021, **7**, 310–319.
10. P. Giannozzi, S. Baroni, N. Bonini, M. Calandra, R. Car, C. Cavazzoni, D. Ceresoli, G. L. Chiarotti, M. Cococcioni, I. Dabo, A. Dal Corso, S. de Gironcoli, S. Fabris, G. Fratesi, R. Gebauer, U. Gerstmann, C. Gougoussis, A. Kokalj, M. Lazzeri, L. Martin-Samos, N. Marzari, F. Mauri, R. Mazzarello, S. Paolini, A. Pasquarello, L. Paulatto, C. Sbraccia, S. Scandolo, G. Sclauzero, A. P. Seitsonen, A. Smogunov, P. Umari and R. M. Wentzcovitch, *J. Phys. Condens. Matter Inst. Phys. J.*, 2009, **21**, 395502.
11. J. Noffsinger, F. Giustino, B. D. Malone, C.-H. Park, S. G. Louie and M. L. Cohen, *Comput. Phys. Commun.*, 2010, **181**, 2140–2148.
12. X. Li, Z. Zhang, J. Xi, D. J. Singh, Y. Sheng, J. Yang and W. Zhang, *Comput. Mater. Sci.*, 2021, **186**, 110074.
13. X. Shi, J. Yang, J. R. Salvador, M. Chi, J. Y. Cho, H. Wang, S. Bai, J. Yang, W. Zhang and L. Chen, *J. Am. Chem. Soc.*, 2011, **133**, 7837–7846.
14. P. F. Qiu, J. Yang, R. H. Liu, X. Shi, X. Y. Huang, G. J. Snyder, W. Zhang and L. D. Chen, *J. Appl. Phys.*, 2011, **109**, 063713.